Carbohydrate Polymers 95 (2013) 303–314

Contents lists available at SciVerse ScienceDirect

Carbohydrate Polymers

journal homepage: www.elsevier.com/locate/carbpol

Ethylenediaminediacetic acid bis(carbido amide chitosan): Synthesis and evaluation as solid carrier to fabricate nanoemulsion

Kuldeep Singh, A.K. Tiwary, Vikas Rana*

Pharmaceutics Division, Department of Pharmaceutical Sciences and Drug Research, Punjabi University, Patiala 147002, India

ARTICLE INFO

Article history:
Received 30 October 2012
Received in revised form 17 February 2013
Accepted 18 February 2013
Available online 6 March 2013

Keywords:
Solid/liquid preconcentrated nanoemulsion
Primaquine
Microparticles
Chitosan derivatives
Spray drying
Ethylenediaminediacetic acid bis(carbido amide chitosan)

ABSTRACT

We have optimized the synthesis of spray dried ethylenediaminediacetic acid bis(carbido amide chitosan) (ED-chitosan) microparticles employing 3^2 full factorial design. The ED-chitosan microparticles were characterized using FTIR-ATR, DSC analysis, oil adsorbing capacity, oil desorbing capacity, surface free energy and dynamic advancing contact angle. The ED-chitosan microparticles were found to have enhanced dispersive component of surface free energy as compared to Aerosil 200. However, they showed lower polar component. This was associated with similar oil adsorbing capacity but higher desorbing capacity. The SEM analysis supported ability of ED-chitosan microparticles to completely spread lipophillic drug over its surface. The reconstituted nanoemulsion generated from ED-chitosan was stable (neutral zeta potential), spherical shaped and 110 nm size (TEM analysis). Further, these nanoemulsions when prepared with primaquine were successfully enhanced *in vitro* dissolution and its *ex vivo* performance. Thus, the study showed new possibilities of industrial acceptance of ED-chitosan microparticles as a solid carrier for the fabrication of nanoemulsion.

1. Introduction

Polysaccharides of natural origin and their derivatives have received great acceptance by pharmaceutical and food industry due to their safety, biodegradability, biocompatibility and non toxicity (Bernkop-Schnurch, 2000; Muzzarelli et al., 2012). They are widely used as thickening agent, gelling agent, emulsifying agent, binding agent, encapsulating agent, swelling agent, disintegrating agent, foam stabilizer, *etc* (Ferrari et al., 2013; Rana et al., 2011; Schafroth, Arpagaus, Jadhav, Makne, & Douroumis, 2012). Further, chemical modifications of polysaccharides have been employed to improve their properties as a biopolymer (Kumar, Muzzarelli, Muzzarelli, Sashiwa, & Domb, 2004). Carboxymethylation/carbamoylethylation, grafting with acrylic acid or its derivatives, thiolation, amination, *etc.* were used as a tool to widen the application of polysaccharides (Jindal, Kumar, Rana, & Tiwary, 2013; Muzzarelli & Ilari, 1994; Muzzarelli, Greco, Busilacchi, Sollazzo, & Gigante, 2012b).

Solid preconcentrated nano/microemulsion (S-PCN) is the delivery system which contains liquid preconcentrated nano/microemulsion adsorbed (or dispersed/merged) over solid substrate. Such delivery systems were advantageous in terms of improved dissolution, enhanced oral bioavailability of poorly water soluble drugs, better oral dosage forms, *etc.* Further, amongst excipients used in the fabrication of S-PCN, solid substrate is the most important excipient. The ideal solid carrier is that which has an ability to carry enhanced amount of lipid and same amount should be released when required. Planinsek, Kovacic, and Vrecer (2011) reported low density porous carriers with large surface area composed of porous silica (Sylysia®) as well as magnesium aluminometasilicate (Neusilin®) in order to improve dissolution and bioavailability of poorly soluble drugs such as carvedilol, indomethacin. Kang, Oh, Oh, Yong, and Choi (2012) used various solid carriers of different properties, *i.e.* hydrophobic (silicon dioxide, magnesium sterate) and hydrophilic (PVA, Na-CMC and HP-β-CD). All of these carriers had significant and positive effects on the crystalline properties, dissolution rate and oral bioavailability of flurbiprofen in the solid-PCN. Aerosil 200, D-mannitol, Gelatin, microcrystalline cellulose and Lactose were also employed as solid carriers in various formulations of solid-PCN (Kang et al., 2012; Shanmugam et al., 2011; Tang, Cheng, Gu, & Xu, 2008). However, these solid carriers provide lower oil carrying capacity, low bulk density, lower compressibility such that their dosage form could not be made. Hence, an attempt was made to develop a solid carrier that could easily entrap enhanced amount of lipid phase (containing poorly water soluble drug) to form preconcentrated nanoemulsion.

Spray drying of chitosan salt solution is now a routine technique to prepare microspheres (Muzzarelli, Stani, Gobbi, Tosi, & Muzzarelli, 2004; Mohajel et al., 2012). The microspheres

* Corresponding author. Tel.: +91 9872023038.
E-mail address: vikas_pbi@rediffmail.com (V. Rana).

0144-8617/$ – see front matter © 2013 Elsevier Ltd. All rights reserved.
http://dx.doi.org/10.1016/j.carbpol.2013.02.030

prepared were in the size range of 2–5 μm. These microspheres were free flowing powder, compressible and therefore most suitable as drug carrier (Rege, Garmise, & Block, 2003a; Rege, Garmise, & Block, 2003b). In addition, spray drying of chitosan salts at various inlet temperature 70–160 °C provides chitosan microsphere varies in their solubility as well as swelling characteristics (Muzzarelli et al., 2004). However, preparation of spraying solution to prepare chitosan microspheres is a tedious task. Chitosan in acetic acid solution reacts immediately with its polyanionic agents (alginic acid, carboxy methylcellulose, acacia gum, *etc.*) to form gelatinous precipitates (Cervera et al., 2011). These gelatinous precipitates were unable to spray dry. Therefore, chitosan carbamate salt in alkaline medium was prepared to obtain clear solution with polyanion (Bernkop-Schnurch & Scerbe-Saiko, 1998). Hence, an attempt was made to identify a polyanionic agent that form clear solution in acetic acid solution of chitosan. This could avoid the formation of chitosan carbamate step necessary for the formation of chitosan microspheres. Chitosan in acetic acid was reported to forms a clear solution with EDTA-diNa (Singh, Suri, Tiwary, & Rana, 2012). Thus, spray drying of chitosan EDTA clear solution shall be expected to form microparticles having enhanced hydrophobic surface as compared to chitosan acetates microparticles. Further, various attempts have been made to encapsulate drugs into the chitosan microspheres prepared by spray drying technology (Schafroth et al., 2012). However, this technology was not found suitable for poorly water soluble drugs and drugs sensitive to temperature. Thus, for such drugs an alternative would be to utilize the surface of microparticles prepared after spray drying shall be subjected to drug adsorption in lipid phase under room temperature. For this purpose, the microparticles should have enhanced hydrophobic surface (Cui, Shi, Zhang, Tao, & Kawashima, 2006). Therefore, a need was felt to prepare microparticles *via* amide linkages to form interpenetrating network that provide microparticles with hydrophobic surface.

In the light of the above, the present investigation was aimed to optimize the synthesis of ethylenediaminediacetic acid bis(carbido amide chitosan) (ED-chitosan) microparticles without the use of proton initiator. The synthesized ED-chitosan microparticles were characterized and evaluated for the fabrication of solid preconcentrated nanoemulsion (S-PCN).

2. Materials and methods

2.1. Materials

Primaquine diphosphate was supplied from Indswift Ltd. (Panchkula, India). Chitosan (88–89% deacetylated) was purchased from India Sea Foods (Cochin, India). Acetic acid, ethylenediaminetetraacetic acid disodium salt (Loba Chemie, Bombay, India) and isopropyl alcohol were used as supplied. All other chemicals used were of analytical grade and used as received.

2.1.1. Synthesis of ethylenediaminediacetic acid bis(carbido amide chitosan)

The ED-chitosan was synthesized employing spray drier without the use of proton initiator. For the synthesis, chitosan was dissolved in 1 N HCl or acetic acid. Separately, ethylenediaminetetraacetic acid disodium salt (EDTA-diNa) was dissolved in 50 mL distilled water. Chitosan solution was added dropwise to EDTA-diNa solution with constant stirring at 2000 rpm. This clear solution was spray dried using a laboratory scale spray drier (Labultima India, Mumbai, India) equipped with a standard 1 mm nozzle. The specifications (inlet temperature = 70–170 °C, cool temperature = 30 °C, inlet high temperature = 185 °C, outlet high temperature = 175 °C, aspirator flow rate = 40 Nm^3/h and feed rate = 1 mL/min) were used to spray dry the chitosan-EDTA-diNa solution. The product obtained after spray drying contained both water soluble and water insoluble microparticles. Therefore, microparticles were suspended in double distilled water. The water insoluble microparticle fraction was recovered as pellet after centrifugation (5000 rpm for 30 min). The water soluble microparticle fraction was obtained after freeze drying the supernatant. The control chitosan microparticles were also prepared by dissolving chitosan in acetic acid and spraying this solution as reported above.

2.1.2. Experimental design

3^2 Full factorial design was selected to optimize synthesis of ED-chitosan. During preliminary studies, proportions of chitosan to EDTA and inlet temperature of spray drier were found to be the critical factors (dependent variables). Percentage yield of water soluble (Y_1)/insoluble fractions (Y_2) of spray dried powder were independent variables.

2.2. Identification of different fractions

2.2.1. FTIR-ATR analysis

A pure sample of chitosan, EDTA-disodium, water soluble/insoluble fractions were subjected to FTIR-ATR analysis (RXI-JR, Alpha-E, Bruker, Germany) in the spectral region of 500–4000 cm^{-1}.

2.2.2. DSC analysis

Differential scanning calorimetric thermogram of chitosan, EDTA-disodium, water soluble/insoluble fractions were recorded using differential scanning calorimeter (Q10, TA Systems, USA) in the temperature range of (40–400 °C) at a heating rate of 10 °C per minute in nitrogen atmosphere (50 mL/min).

2.3. Characterization of ED-chitosan

2.3.1. Oil adsorbing capacity (OAC) of ED-chitosan

For the estimation of OAC, ethanolic solution of soyabean oil, labrafac PG, Soyabean oil:Tween 80 (70:30) and Labrafac PG:Tween 80 (70:30) were prepared. These ethanolic solutions of oil with or without Tween 80 were mixed with 1gm of ED-chitosan. The OAC was estimated by weighing the pure ED-chitosan (W_a) or control chitosan microparticles and weight of dried ED-chitosan (W_b) or control chitosan microparticles obtained after the evaporation of ethanol from the blend of ED-chitosan and ethanolic solution of soyabean oil, labrafac PG, Soyabean oil:Tween 80 (70:30) and Labrafac PG:Tween 80 (70:30). The inclusion criterion for the W_b was on the basis of initial screening of powder blend. Only those ED-chitosan or control chitosan microparticles/Oil:Tween 80 powder blends obtained after evaporation of ethanol that showed no significant changes in physical properties as that of pure ED-chitosan such as non oily, non sticky, free flowing and with similar texture as that of pure ED-chitosan was accepted for W_b.

The OAC was estimated by the formula

$$\text{OAC} = \frac{W_b - W_a}{W_a} \times 100$$

2.3.2. Oil desorbing capacity (ODC) of ED-chitosan

The oil desorbing capacity was estimated by suspending oil adsorbed ED-chitosan or control chitosan microparticles (W_b) in 10 mL of water. After stabilization for 1 h, the suspended particles were recovered by centrifugation (3000 rpm/min), dried and weighed (W_c). The ODC was estimated by the formula

$$\text{ODC} = \frac{W_b - W_c}{W_c} \times 100$$

2.3.3. Surface free energy components of ED-chitosan/Aerosil 200

The surface free energy components of ED-chitosan or control chitosan microparticles or Aerosil 200 were estimated as per the method reported by Chibowski and Perea-Carpio (2001). The dispersive and polar components of surface free energy of ED-chitosan or control chitosan microparticles or Aerosil 200 before and after oil adsorption were estimated employing diiodomethane ($\gamma_l^{lw} = 50.8$, $\gamma_l^+ = 0$, $\gamma_l^- = 0$); *n*-hexane ($\gamma_l^{lw} = 18.4$, $\gamma_l^+ = 0$, $\gamma_l^- = 0$), dimethylsulphoxide (DMSO; $\gamma_l^{lw} = 36$, $\gamma_l^+ = 0.5$, $\gamma_l^- = 32$) and water ($\gamma_l^{lw} = 21.8$, $\gamma_l^+ = 25.5$, $\gamma_l^- = 25.5$) as probe liquids. The advancing weight as well as reducing weight for each probe liquid obtained were incorporated into following equation to determine dispersive and total polar components.

$$W_a = 2[(\gamma\gamma_l^{LW})^{1/2} + (\gamma_s^+\gamma_l^-)^{1/2} + (\gamma_s^-\gamma_l^+)^{1/2}]$$

where, W_a is the work of adhesion of the liquid to the solid surface, where γ_s^{lw} is the dispersive (apolar Lifshitz–van der Waals), γ^+ electron acceptor, and γ^- is the electron donor interactions.

2.3.4. Dynamic advancing contact angle

The dynamic advancing contact angle (θ_a) was estimated as per the method reported by Chibowski and Perea-Carpio (2001) and it is different from contact angle on a flat surface of same solid. For the estimation of θ_a, two components namely advancing weight of the probe liquid (water) in the capillary (m_a) and effective pore radius of the solid ($R_{eff.p}$) were determined. The m_a of ED-chitosan or Aerosil 200 before or after oil adsorption was estimated by weighing 0.200/0.400 g and transfer to micropipette tips. These filled micropipette tips were dipped in to 2–3 mm layer of the probe liquid (water) in a vessel. When the top bed of the micropipette tips became wetted with the liquid, the tip was weighted (m_a) again to find the amount of the liquid taken in by the powder. Reff.p of the powder blend was estimated according to the method reported by Rai, Tiwary, and Rana (2012). In brief, the micropipette tip (2 mL, transparent) was filled with the powder and weighed (W_A). Then *n*-hexane [surface tension (γ) 18.4 mN/m] was poured dropwise on the bedtop till the solvent filtered out at the bottom of the tip. The tip was weighed again (W_B). The experiments were repeated six times. Following equation was used to estimate Reff.p.

$$R_{eff.p} = \frac{W_A - W_B}{2\pi\gamma}$$

Thus, the following equation was used to estimate θ_a

$$\text{Cos}\,\theta_a = \frac{m_a g}{2\pi R_{eff.p}\gamma}$$

where $g = 980\ \text{cm/s}^2$ and $\gamma = 72.6$ dyn/cm.

2.4. Fabrication of ED-chitosan solid preconcentrated nanoemulsion (ED-chitosan-S-PCN)

Primaquine diphosphate was converted into lipid soluble primaquine base (PQ) by precipitation method as reported by Singh and Vingkar (2008). For the preparation of ED-chitosan-S-PCN, PQ was dissolved in lipid phase (soyabean oil:Tween 80::70:30). 5 mL of 10% (v/v) of lipid phase in ethanol was adsorbed on ED-chitosan microparticles (1 gm). The ethanolic solution of lipid phase was prepared for the uniform distribution of lipid phase into ED-chitosan. The excess ethanol if present was evaporated on water bath to form ED-chitosan-S-PCN microparticles. The dried ED-chitosan-S-PCN microparticles powder obtained was stored in polyethylene bags till further use. A similar method was used to prepare Aerosil 200-S-PCN (A standard carrier generally used for the preparation of S-PCN) instead of ED-chitosan.

2.5. Evaluation of ED-chitosan-S-PCN

2.5.1. Morphological evaluation

The outer macroscopic structure of ED-chitosan and ED-chitosan-S-PCN, Aerosil 200 and Aerosil 200-S-PCN was investigated by scanning electron microscopy (S-4100, Hitachi, Japan) at 15 keV accelerating voltage. The sample was fixed on a SEM-stub using double-sided adhesive tape and then coated with a thin layer of gold.

2.5.2. Flow properties

The flow properties (loosely packed bulk density, tapped bulk density, compressibility index, hausner ratio and angle of repose related directly with the behaviour of the powdered products during storage, manipulation and posterior processing. In general, the processing parameters have significant effect on these properties. The flow properties of ED-chitosan microparticles, ED-chitosan-S-PCN, Aerosil 200 and Aerosil 200-S-PCN were characterized for angle of repose, bulk density, tapped density, Carr's index (%), and Hausner ratio as reported earlier (Rattes & Oliveira, 2007).

2.5.3. Evaluation of reconstituted nanoemulsion obtained from ED-chitosan-S-PCN/Aerosil 200-S-PCN

100 mg of ED-chitosan-S-PCN/Aerosil 200-S-PCN was suspended in 10 mL of water with constant stirring. The suspension was centrifuged at 5000 rpm for 10 min to separate solid undissolved components. The supernatant obtained was reconstituted nanoemulsion.

2.5.4. Determination of droplet size, size distribution and zeta potential

The particle size of the reconstituted nanoemulsion was determined by Zetasizer Nano ZS (Malvern Instruments, UK) at a wavelength of 635 nm and scattering angle of 90° at 25 °C. Each study was carried out in triplicate to ensure reproducibility.

2.5.5. Transmission electron microscopy

Morphological and structural examination of ED-chitosan microparticles/Aerosil 200 suspended in water and reconstituted solution in water prepared from ED-chitosan-S-PCN/Aerosil 200-S-PCN was carried out using transmission electron microscopy (TEM; Hitachi, Tokyo, Japan) on an H7500 machine operating at 100 kV capable of point-to-point resolution. A 0.5 mL droplet of these samples was directly positioned on the copper electron microscopy grids, stained with 0.5% (w/v) aqueous solution of phosphotungstic acid for 30 s, and the excess was drawn off. The grids were then observed by TEM after drying. Combinations of different bright-field imaging at increasing magnification were used to expose the structure as well as the size of the formed oil droplets/solid ED-chitosan microparticles/Aerosil 200.

2.5.6. Stability testing of reconstituted nanoemulsion

The stability of reconstituted nanoemulsion was examined using emulsification time determination, thermodynamic stability studies and cloud point measurements as per the method reported by Elnaggar, El-Massik, and Abdallah (2009) and Bandyopadhyay, Katare, and Singh (2012) respectively.

2.6. In vitro dissolution studies

PQ released from ED-chitosan-S-PCN/Aerosil 200-S-PCN was evaluated by using the US pharmacopoeia dissolution apparatus II-paddle (Electrolab india, Mumbai, India) at 37 ± 0.5 °C using 500 mL of 0.1 N HCl as a dissolution medium with stirring speed of 50 rpm. Aliquots (5 mL) withdrawn at various time intervals were immediately filtered through whatman filter paper, diluted suitably

and analyzed for PQ spectrophotometrically (Beckman DU-640 B UV–vis spectrophotometer) at 265 nm.

2.7. Ex vivo permeation studies

The enhancement in the transportation of PQ across biological membrane (porcine small intestine) was examined when PQ was entrapped into nanoemulsion fabricated either from ED-chitosan or from Aerosil 200. For this purpose, porcine small intestine was used as diffusional barrier (Ghai & Sinha, 2012). Porcine small intestine was procured from a local slaughter house and used within 1 h of slaughter. The tissue was stored in Kreb's Ringer phosphate buffer (KRPB) at 4 °C continuously aerated with the aid of an electrical aerator. A 10 cm length of porcine small intestine was excised, washed using saline and placed on saline-soaked filter paper. The isolated intestinal tract was cut lengthwise to flatten it using scissors. The serosal membrane inside was set upward using a filter paper, with the help of a scalpel, the muscle layer was removed. The intestinal membrane was tied to one side of the open tube and this side of the tube (donor compartment) was submerged carefully in a beaker containing 22.5 mL of phosphate buffer pH 6.8 (receptor compartment). Phosphate buffer was stirred at 50 rpm and maintained at 37 ± 0.5 °C. Subsequently, a total of 225 mg ED-chitosan-S-PCN/Aerosil 200-S-PCN formulations were added from the top of the tube (donor compartment) at the mucosal side of isolated intestine (each experiment was performed in triplicate). Aliquots of 1 mL samples were withdrawn at different time intervals and replaced with fresh 1 mL buffer each time maintained at 37 ± 0.5 °C in the receptor compartment. The amount of PQ diffused across porcine small intestine was determined spectrophotometrically at 265 nm after appropriate dilutions.

3. Results and discussion

3.1. Synthesis of ED-chitosan

Chitosan form soluble salts with acetic acid. However, chitosan dissolved in acetic acid immediately react with sodium salts of organic acids to produce white gelatinous precipitates. Moreover, EDTA is insoluble in acidic conditions below pH 4.3–4.7. Thus, disodium salt of ethylenediaminetetra acetic acid was chosen. The addition of EDTA disodium salt solution into chitosan actetae solution leading gelatinous precipitates after sometime. Therefore, dropwise addition of EDTA disodium salt solution into chitosan acetate solution under vigorous stirring at 2000 rpm provides clear ionic solution of chitosan and EDTA. This clear chitosan-EDTA solution was spray dried to obtain microparticles. Thus, the method is simple and avoids formation of chitosan carbamates step necessary to obtain clear spraying solution (Bernkop-Schnurch & Scerbe-Saiko, 1998). During preliminary investigations, it was evident that spray drying of chitosan-EDTA solution with variable concentration and temperature produce mixture of water soluble fraction and water insoluble fraction. Thus, to optimize the process for the synthesis of ED-chitosan, 3^2 full factorial design was applied.

An experimental design can be defined as the strategy for setting up experiments in such a manner that the information required could be gathered efficiently and precisely as possible. Therefore, two factor and each factor at three levels (3^2 full factorial design) was used for the synthesis of ED-chitosan. The experimental trials were performed for all 9 possible combinations. The proportions of chitosan:EDTA (X_1) and inlet temperature of spray drier (X_2) were identified as the active independent factors influencing the synthesis of water insoluble fraction (Y_2) and the byproduct water soluble fraction (Y_1) both taken as dependent variables. The experimental trials conducted were summarized in Table 1. A statistical

Table 1
3^2 Full factorial design for the synthesis of ED-chitosan microparticles.

Codes	Independent variables	Level			Codes	Dependent variables	Level		Objective
		Low (−1)	Middle (0)	High (+1)			Low	High	
Detail of variables									
X_1	Proportion of CH to EDTA disodium salt	60:40	50:50	40:60	Y_1 (%)	Yield of water soluble fraction	2.03 ± 0.02	38.11 ± 1.1	Minimum
X_2	Inlet temperature (°C) of spray drier	70	120	170	Y_2 (%)	Yield of water insoluble fraction	40.02 ± 0.9	40.02 ± 1.2	Maximum
3^2 Full factorial design									
Experimental trials		S2	S3	S4	S5	S6	S7	S8	S9
X_1		−1	−1	0	0	0	1	1	1
X_2		−1	1	−1	0	1	−1	0	1
Y_1[a]		32.61 ± 1.3	28.63 ± 0.9	25.32 ± 0.9	9.54 ± 0.6	7.52 ± 0.6	2.03 ± 0.07	38.11 ± 1.2	31.31 ± 1.1	29.31 ± 1.2
Y_2[a]		7.52 ± 0.54	17.91 ± 0.8	19.32 ± 0.6	25.0 ± 1.1	28.52 ± 0.8	46.0 ± 1.4	3.72 ± 0.02	7.21 ± 0.8	10.21 ± 0.9
Coefficients									
Codes of dependent variables	Intercept		X_1	X_2	X_1^2	X_2^2	X_1X_2		
Y1	6.12		2.05	−3.92	+24.52	0.32	−0.4		
Y2	32.66		−3.92	6.57	−22.18	+0.77	−1.3		

[a] Values are mean ± SD (n = 6).

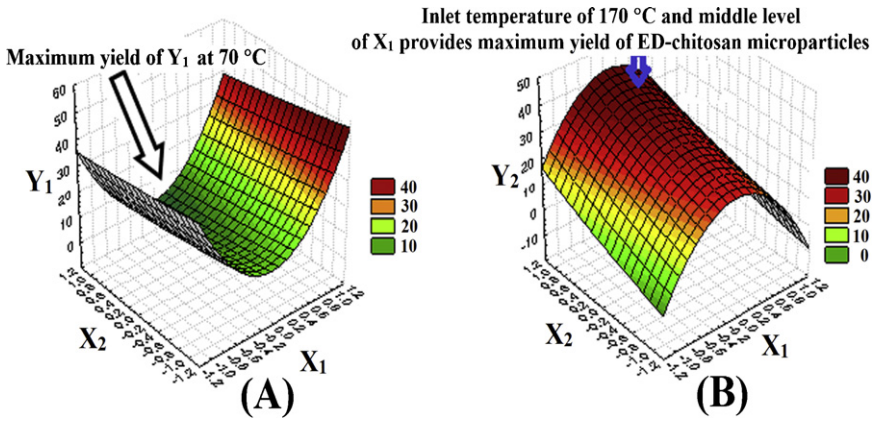

Fig. 1. Response surface plot showing correlation of proportions of chitosan:EDTA (X_1) and inlet temperature of spray drier (X_2) with; (A) water soluble fraction; (B) water insoluble fraction.

model incorporating interactive and polynomial terms were used to evaluate responses.

$$Y = b_o + b_1X_1 + b_2X_2 + b_3X_1X_2 + b_4X_1^2 + b_5X_2^2$$

where b_o is the intercept representing the arithmetic average of quantitative outcome of 9 experimental trials. b_1 and b_2 are the coefficient computed from the observed experimental value of Y_1/Y_2. X_1 and X_2 are the coded level of the independent variable (Table 1). The main effects (X_1 and X_2) represent the average results of changing 1 factor at a time from its low to high value. The interaction terms (X_1 and X_2) show how the response changes when two factors are simultaneously changed. The polynomial terms (X_1^2 and X_2^2) are included to investigate nonlinearity.

The results obtained after 9 experimental trials were subjected to multiple linear regression analysis. Following quadratic equation were generated depicting correlation of yield of water soluble fraction/water insoluble fraction with process variables (Table 1).

Percentage yield of water soluble fraction $= 6.122 + 2.05X_1 + 24.52X_{12} - 0.4X_1X_2 + 0.3167X_2^2$

Percentage yield of water insoluble fraction $= 32.66 - 3.92X_1 + 6.566X_2 - 22.18X_1^2 - 1.3X_1X_2 + 0.77X_2^2$.

The coefficients (b_1 and b_2) associated with the effect of various process variables on percentage yield of water soluble fraction/water insoluble fraction are shown in Table 1. The negative sign of coefficients signifies an antagonistic effect while a positive sign of coefficients signifies a synergistic effect. Therefore, the coefficients generated after multiple linear regression revealed increase in the proportion of chitosan:EDTA from 60:40 to 40:60 increased the yield of water soluble fraction and decreased the water insoluble fraction. However, antagonistic effect of quadratic terms (X_1^2 and X_1X_2) enhanced the percentage yield of water insoluble fraction, when 50:50 chitosan:EDTA proportion was used for synthesis (Fig. 1A). The significantly higher and synergistic contribution of b_2 (coefficient of X_2) obtained with water insoluble fraction as compared to negative value of b_2 of Y_1 suggested higher inlet temperature of 170 °C was necessary to prepare water insoluble fraction with enhanced yield. On the other hand, lower level of inlet temperature (70 °C) produces water soluble fraction. Overall, to achieve a water insoluble fractions with higher yield it was necessary to set the inlet temperature of spray drier to 170 °C, cool temperature = 30 °C, aspirator flow rate = 40 Nm^3/h and flow rate of 1 mL/min and equal proportion of chitosan and EDTA disodium (Fig. 1B).

In a conventional method, free radical initiator was used to form active ester intermediate (Bernkop-Schnurch & Krajicek, 1998). The intermediate can react with primary amine of chitosan to form an amide linkage. A various different free radical initiators like ammonium persulfate, potassium persulfate, ceric ammonium nitrate, EDAC (1-ethyl-3-(3-dimethylaminopropyl)carbodiimide hydrochloride, thiocarbonation potassium bromate, potassium diperiodatocuprate (III), 2,2-azobisisobutyronitrile, ferrous ammonium sulfate and genipin have been explored for amide conjugation (Alves & Mano, 2008; Muzzarelli, 2009). A chitosan covalently crosslinked with EDTA was prepared using free radical initiator and was found to show mucoadhesive, antibacterial and antifungal properties (Bernkop-Schnurch & Krajicek, 1998; El-Sharif & Hussain, 2011; Loretz & Bernkop-Schnürch, 2006). However, these free radical initiator techniques sometimes cause degradation of the polysaccharide backbone, giving rise to the products with complicated and ambiguous structures. Qu, Wirsen, and Albertsson (1999) have reported the amide conjugation of chitosan and D,L Lactic acid first at 80 °C for 4 h to avoid evaporation of the monomer then put under a vacuum at 80 °C for 3 h to promote dehydration of the chitosan copolymer salts with formation of the corresponding amide linkages. Thus, spray drying method presented was advantageous with respect to its simplicity, no chance of degradation of polysaccharide backbone and without the use of any proton initiator.

3.2. Identification of water soluble/insoluble fractions

The FTIR analysis was conducted to determine the molecular level difference in water soluble or insoluble fraction. FTIR spectra of water insoluble fraction, the reactants and the byproducts are shown in Fig. 2. The FTIR spectra of chitosan (Fig. 2A) showed a broad —OH stretching absorption band between 3450 cm^{-1} and 3100 cm^{-1} and the C—H stretching between 2990 cm^{-1} and 2850 cm^{-1}. Another major absorption band observed between 1220 cm^{-1} and 1020 cm^{-1} represents the free amino group ($—NH_3^+$) at C2 of glucosamine, a major group present in chitosan. Peak at 1610 cm^{-1} representing acetylated amino group of chitosan indicated that the sample was not fully deacetylated. The FTIR spectra of EDTA disodium showed a broad —OH stretching absorption band 3450 cm^{-1}–3100 cm^{-1} and absorption peaks at 2586 cm^{-1} and 2451 cm^{-1} representing —OH stretching of carboxylic acid (Fig. 2B). Absorption

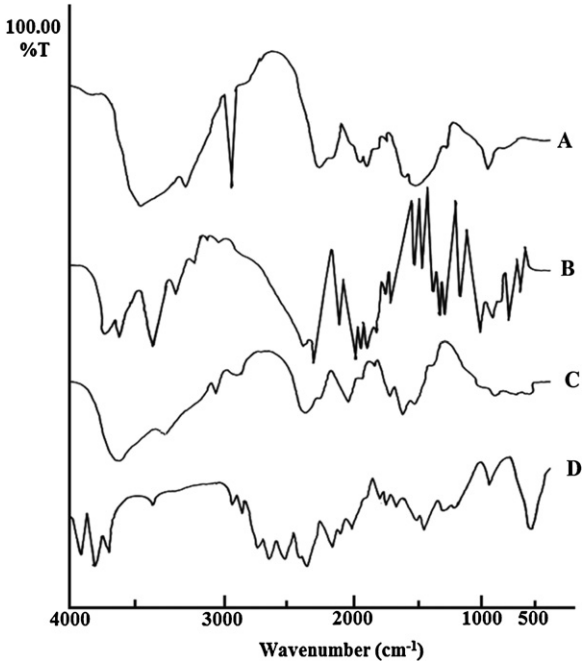

Fig. 2. FTIR spectra of chitosan powder (A); EDTA disodium salt (B); chitosan-EDTA PEC (C); ED-chitosan (D).

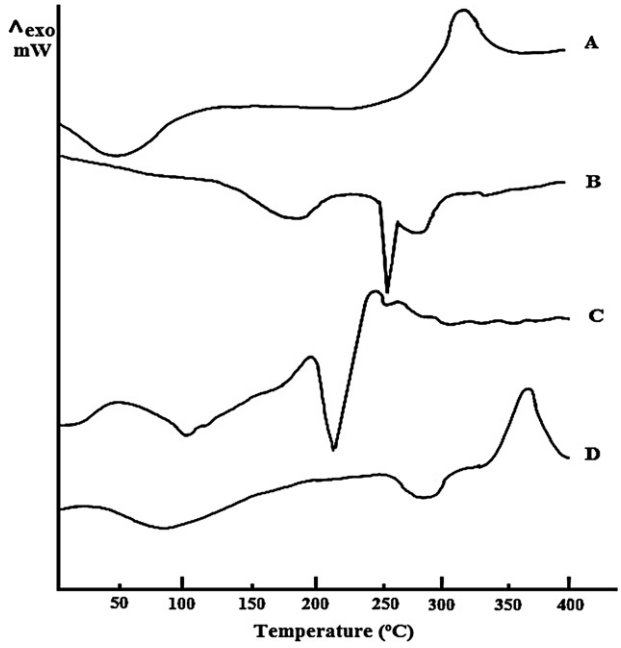

Fig. 3. DSC thermogram of chitosan powder (A); EDTA disodium salt (B); chitosan-EDTA PEC (C); ED-chitosan (D).

peaks at 1673 cm^{-1} representing —C=O stretching, 1476 cm^{-1} representing CH_2 bending and 1395 cm^{-1} representing —OH bending were also present in EDTA sample. A chitosan-EDTA PEC was prepared by mixing chitosan solution (prepared in 3%, w/v, acetic acid) with EDTA in water followed by precipitation in isopropyl alcohol. These precipates were dried in oven at 50 °C for 72 h and then microwave dried (85 W, 15 s 10 cycles) to remove any bound water (Singh et al., 2012). Prominent peaks at 1635 cm^{-1} of $—NH_3^+$ of chitosan, 1406 cm^{-1} symmetric stretch of $—COO^-$ moieties of EDTA were observed. Weak peak at 1255 cm^{-1} of carboxylic acid (—COOH) moieties of EDTA indicated that all the —COOH moieties of EDTA had not interacted with all the $—NH_3^+$ group of chitosan. This was further evident by the occurrence of a weak peak at 2925 cm^{-1} that indicates free acetate moieties present in chitosan-EDTA PEC sample (Singh et al., 2012). The FTIR spectra of water soluble fraction showed a similar peak at 1635 cm^{-1} (of NH_3^+) of chitosan, 1406 cm^{-1} (symmetric stretch of COO^-) as observed in chitosan-EDTA PEC (Fig. 2C). Thus, the water soluble fraction was identified as chitosan-EDTA PEC. Fig. 2D showed FTIR spectra of sample obtained from water insoluble fraction that exhibited peaks at 1645 cm^{-1} characteristic of amide linkage. However, the occurrence of peak at 2367 cm^{-1} suggested presence of free acetate moieties. Thus, supported all the acetate moieties had not participated in the amide linkage. This indicated that the water insoluble fraction was identified as Ethylenediaminediacetic acid bis(carbido amide chitosan) (ED-chitosan). Further the DSC analysis was performed to understand the purity of synthesized products. The DSC thermogram of water soluble fraction obtained after freeze drying showed characteristic peaks at 215 °C indicated for chitosan-EDTA PEC (Singh et al., 2012). However, the water insoluble fraction (ED-chitosan) showed endothermic transition at 321.03 (Fig. 3D) followed by degradation exothermic transition at 375 °C. This supported the purity of ED-chitosan. Therefore, it could be envisaged from DSC and FTIR analysis that ED-chitosan was successfully synthesized employing spray drying technique with an inlet temperature of 170 °C. However, chitosan-EDTA PEC was also formed as a byproduct during the synthesis of ED-chitosan. In addition, decreasing the inlet temperature below 170 °C enhanced the chitosan-EDTA PEC content and decreased the ED-chitosan yield. Fig. 4 shows the structure of chitosan-EDTA PEC and ED-chitosan microparticle.

3.3. Characterization of ED-chitosan

Ideally, a solid carrier should bears the property of high oil adsorbing capacity at its surface and same quantity has been desorbed from its surface with reduced particle size of oil droplets transported into the solvent. Therefore, to explore this property, oil adsorbing capacity and oil desorbing capacity of ED-chitosan was estimated and compared with Aerosil 200 (a standard solid carrier used for preparation of nanoemulsion).

Fig. 5A depicts the results of oil adsorbing capacity and oil desorption capacity of ED-chitosan, control chitosan microparticles and Aerosil 200. The OAC of control chitosan microparticles was minimum as compared to ED-chitosan and Aerosil 200. The results suggested no significant difference ($P > 0.05$) between OAC of ED-chitosan and Aerosil 200 irrespective of lipid phase (Soyabean oil, Labrafac PG, Soyabean oil:Tween 80::70:30 and Labrafac PG:Tween 80::70:30) used to adsorb at the surface of solid carrier (Fig. 5A). However, the ODC of ED-chitosan was found to be enhanced as compare to ODC of Aerosil 200 (Fig. 5A). This suggested ED-chitosan had a capacity to adsorb hydrophobic material and same amount was desorbed from its surface.

To find out this paradoxical surface behaviour of ED-chitosan, surface free energy of ED-chitosan either before or after oil/oil:surfactant adsorption was estimated. Dispersive component of surface free energy is an indicator of hydrophobic surface. The polar component of surface free energy is a reflection of hydrophilic surface. This concept of surface free energy was applied by Matsumaru (1959) and Yoshihashi, Makita, Yamamura, Fukuoka, and Terada (1998) to explain the correlation of disintegration time of tablets with wetting time of tablets. Therefore, surface free energy component could be used to understand the adsorption/desorption mechanism that had occurred at the surface of ED-chitosan microparticles/Aerosil 200.

The results suggested surface free energy components of control chitosan microparticles and ED-chitosan microparticles were

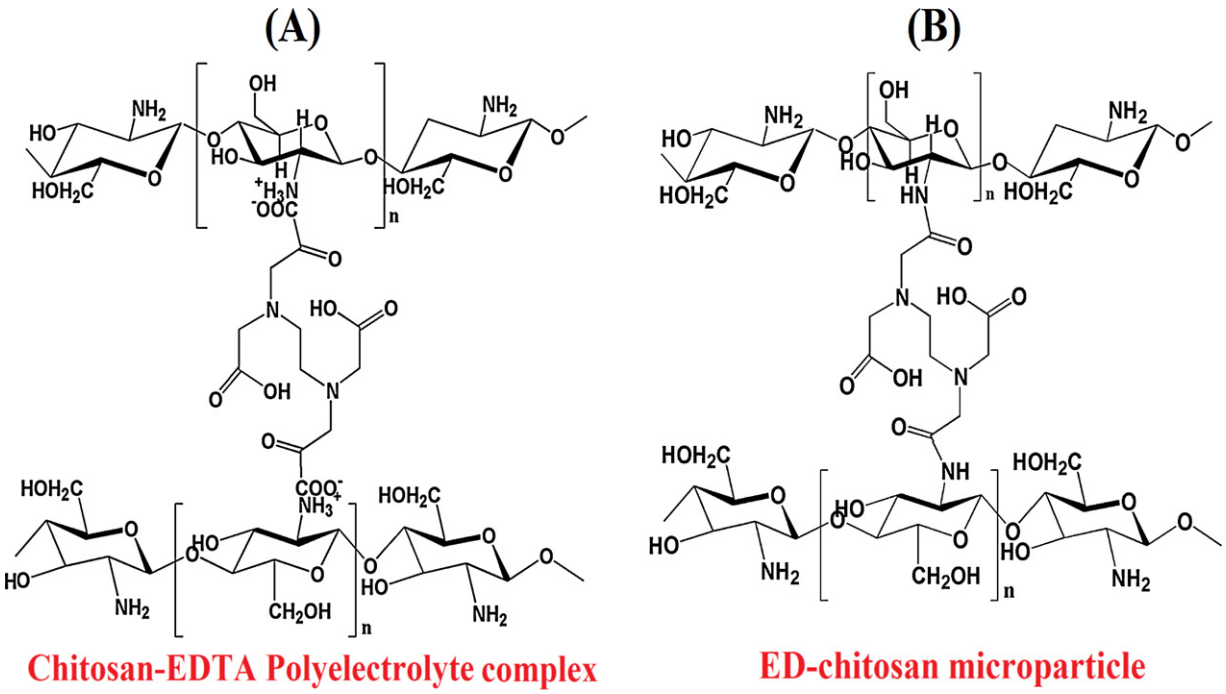

Fig. 4. Structure of chitosan-EDTA PEC (A) and ED-chitosan microparticles (B) prepared by spray drying at different inlet temperatures of spray drier.

respectively $13.2 \pm 1.10\,mJ/m^2$ and $40.43 \pm 1.20\,mJ/m^2$ for dispersive component and $17.97 \pm 1.30\,mJ/m^2$ and $11.57 \pm 0.94\,mJ/m^2$ for polar components. Thus, ED-chitosan microparticles provides hydrophobic surface as compared to control chitosan microparticles. This shows advantage of ED-chitosan microparticles over control chitosan microparticles. In addition, the dispersive component of Aerosil 200 was $46.06 \pm 1.21\,mJ/m^2$ and polar component was $7.26 \pm 0.27\,mJ/m^2$. Interestingly, the adsorption of soyabean oil and labrafac PG over ED-chitosan enhanced the dispersive component and decreased the polar component of ED-chitosan (Fig. 5B). However, adsorption of Soyabean oil:Tween 80/Labrafac PG:Tween 80 mixture on ED-chitosan enhanced polar components and decreased dispersive component (Fig. 5B). In addition, the polar component of lipid phase adsorbed ED-chitosan was higher as compared to Soyabean oil:Tween 80/Labrafac PG:Tween 80 adsorbed Aerosil 200. Thus, enhanced polar component of lipid phase adsorbed ED-chitosan had leads to increased ODC of ED-chitosan as compared to Aerosil 200. This indicates inherent capability of ED-chitosan that had provided sufficient surface free energy necessary for stability of nanoemulsion. In addition, enhanced dispersive component of ED-chitosan after the adsorption of soyabean oil:Tween 80 or Labrafac PG:Tween 80 could reduced the size of oil particles formed after reconstitution of nanoemulsion.

Further, the dynamic advancing contact angle (θ_a) was estimated to understand the surface behaviour (hydrophilic/hydrophobic) of solids (ED-chitosan/Aerosil 200) when comes in contact with water. The findings pointed towards the hydrophobic surface of ED-chitosan. This hydrophobicity was reduced on soyabean oil:Tween 80/Labrafac PG:Tween 80 (70:30) adsorbed ED-chitosan microparticles. However, Aerosil 200 provides hydrophobic surface and this hydrophobicity was enhanced upon adsorption of soyabean oil:Tween 80/Labrafac PG:Tween 80 (70:30) necessary for the development of nanoemulsion (Fig. 5B). This is an indicative of suitability of ED-chitosan in the adsorption and desorption of lipid phases necessary for development of nanoemulsion. Thus, this property of ED-chitosan could be encashed in the formulation development of micro/nanoemulsion.

3.3.1. Surface morphology

Scanning electron microscopy was undertaken to understand the surface characteristics of ED-chitosan microparticle. Fig. 6A showed spherical shaped microparticles in the range of 1–2 μm size. The adsorption behaviour of soyabean oil:Tween 80 mixture over the surface of ED-chitosan microparticles was evident from SEM (Fig. 6B). However, the powder particles of Aerosil 200 were clogged with each other to form aggregates. The origin of these aggregation after addition of lipid phase into powder was probably due to covering of oil globules with powder particles. Further, the size of aggregates may varies due to size of oil droplet developed after addition of oil phase. This suggested ability of spherical shaped micro size ED-chitosan to completely spread lipophillic solvents over its surface that could be employed as an ideal solid carrier to deliver nanoemulsion.

3.3.2. Flow properties

The angle of repose of the synthesized ED-chitosan microparticles remained between 29° and 32°, indicating satisfactory flow properties. As the moisture content of ED-chitosan microparticles was less than 2%, the ED-chitosan microparticles were optimally dried. The other parameters for ED-chitosan microparticles and soyabean oil:Tween 80 (70:30) or labrafac PG:Tween 80 (70:30) adsorbed were also found to be within the acceptable limits. It was quite noticeable that there was no significant difference observed in the flow behaviour of ED-chitosan microparticles and ED-chitosan-SPCN. Aerosil 200 has good flow property yet the free flowing property was decreased Aerosil 200-SPCN. On the other hand, chitosan-EDTA PEC and chitosan-EDTA PEC-SPCN showed poor flow behaviour.

3.4. Exploiting ED-chitosan as a solid carrier for the delivery of preconcentrated nanoemulsion (ED-chitosan-S-PCN/Aerosil 200-S-PCN)

The surface free energy components, oil adsorbing capacity and oil desorbing capacity suggested potential of ED-chitosan for the fabrication of solid preconcentrated nanoemulsion.

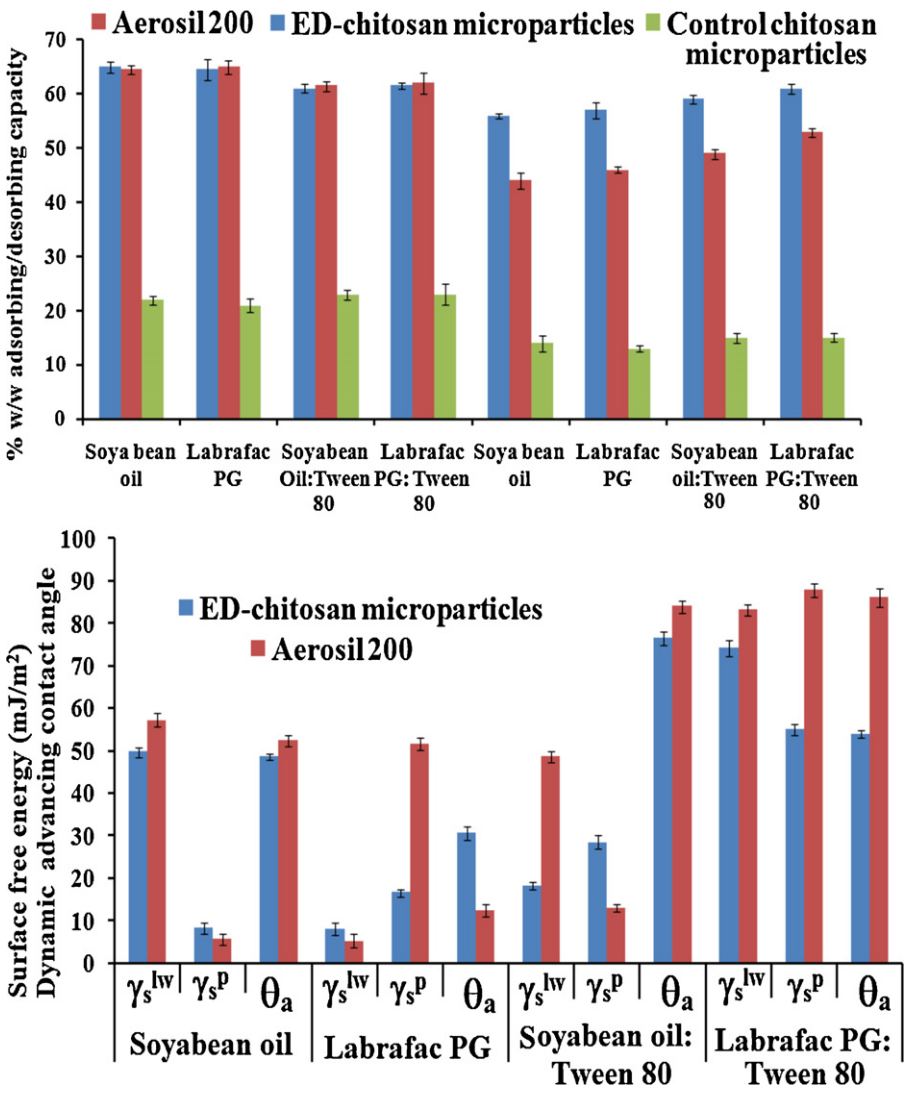

Fig. 5. (A) Oil adsorbing and desorbing behaviour of control chitosan microparticles, ED-chitosan-S-PCN and aerosil 200-S-PCN; (B) surface free energy components of ED-chitosan-S-PCN and aerosil 200-S-PCN.

For this purpose, primaquine (an antimalarial agent) was synthesized from its available primaquine diphosphate salt. The solubility of primaquine was examined in soyabean oil and labrafac PG. To enhance the solubility of primaquine in oils, Tween 80 was screened. In previous studies, Tween 80 has been successfully incorporated into micro/nanoemulsion systems from 30 to 60% with or without cosurfactant (Bachynsky, Shah, Patel, & Malick, 1997; Cho, Kim, Bae, Mok, & Park, 2008; Mehta, Kaur, & Bhasin, 2010). Therefore, lower concentration of Tween 80 was taken to challenge the potential of ED-chitosan/Aerosil 200 to form nanoemulsion. The solubility studies showed 90.51 ± 1.2 mg/mL and 73.83 ± 1.3 mg/mL of primaquine was soluble in soyabean oil:Tween 80 (70:30) and labrafac PG:Tween 80 (70:30), respectively. Therefore, soyabean oil:Tween 80 (70:30) was selected to evaluate ED-chitosan as a solid carrier for nanoemulsion drug delivery system.

In a traditional method drug and solid carrier was mixed and suspended in ethanol (Shanmugam et al., 2011). This ethanolic suspension was spray dried to form solid preconcentrated nanoemulsion. However, in the present investigation ED-chitosan was mixed with soyabean oil:Tween 80, PQ and the ethanolic suspension was subjected to drying on water bath to evaporate ethanol. This method avoids the exposure of PQ to high temperature and hence enhanced stability of drug.

3.5. Evaluation of reconstituted nanoemulsion generated from ED-chitosan-S-PCN/Aerosil 200-S-PCN

3.5.1. Determination of droplet size, size distribution and zeta potential

The droplet size of the emulsion is a critical factor in self nanoemulsification performance because it determines the rate and extent of drug release as well as absorption. The smaller is the droplet size, the larger the interfacial surface area provided for drug absorption. It was observed from Table 2 that the lowest PDI as well as smallest particle size of 110 nm was obtained from reconstituted nanoemulsion generated from ED-chitosan-S-PCN surface as compare to Aerosil 200-S-PCN. The zeta potential is an electrostatic value measured by surface electrostatic double layer of droplets. The neutral zeta potential of reconstituted nanoemulsion generated from ED-chitosan-S-PCN suggested its stability. Thus, the nanoemulsion prepared from ED-chitosan-S-PCN bears nanosize particles. This indicated potential of ED-chitosan to transport primaquine in nanosize droplets.

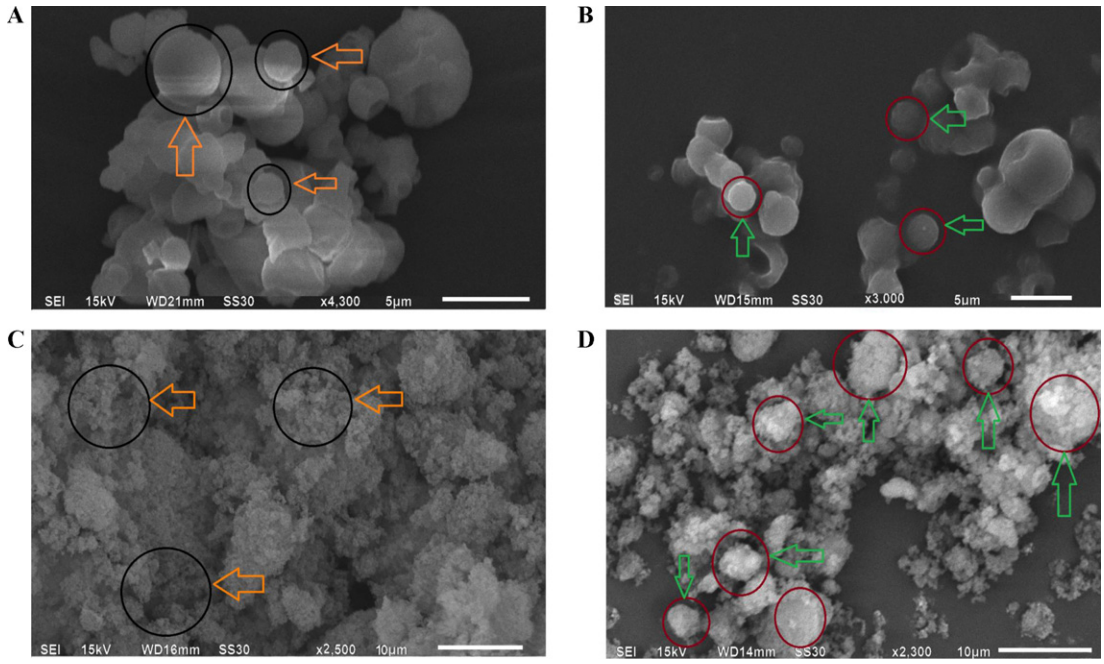

Fig. 6. Scanning electron micrographs of: (A) ED-chitosan microparticles; (B) ED-chitosan-S-PCN; (C) Aerosil 200 (D) Aerosil 200-S-PCN.

3.5.2. Transmission electron microscopy

Fig. 7 shows the TEM images of ED-chitosan/Aerosil 200 and reconstituted nanoemlusion prepared from ED-chitosan-S-PCN/Aerosil 200-S-PCN. The image of ED-chitosan microparticles showed a homogeneous internal morphology suggesting a matrix type structure (Fig. 7A). Aerosil 200 showed aggregates (6–10 μm) formed by smaller primary particles (18.3 nm) and showed similar size as reported earlier (Shah & Thassu, 2005). Fig. 7B and D portray the electron microscopic images depicting the morphology of desorbed nanosize soyabean oil:Tween 80 (70:30) droplets from ED-chitosan-S-PCN and Aerosil 200-S-PCN. As it is evident from Fig. 7B, all the globules formed from ED-chitosan microparticle were of spherical shape, with globule size of nearly 110 nm (Table 2). Further, it was clearly illustrated that there is no signs of coalescence, indicating thereby the enhanced physical stability of the fine droplets formation. Yet the globules formed by Aerosil 200 were spherical in shape, 225 nm size but coalescence was observed which may further proceeds to unstable droplet formation.

3.5.3. Stability testing of reconstituted nanoemulsion

The important criterion for selection of the solid carrier for S-PCN is not only its high oil adsorbing capacity but also the ability of solid carrier to desorb maximum, nanosize and stable oil phase spreaded over its surface. Further, the nature of oil and surfactant phase also affects the stability of nanoemulsion. Therefore, stability testing of reconstituted nanoemulsion was evaluated. The results of stability testing are summarized in Table 2. The ED-chitosan containing soyabean oil:Tween 80 (70:30) was found to disperse quickly (within 28–32 s) and completely when subjected to aqueous environment under mild agitation. This suggested ED-chitosan has an inherent capacity to successfully generate self nanoemulsion when comes in contact with aqueous environment. Further, the cloud temperature, centrifugation and freeze thaw cycle suggested the reconstituted nanoemulsion was found to be thermodynamically stable when generated from ED-chitosan-S-PCN in comparison to Aerosil 200-S-PCN. Thus further pointed towards overwhelming influence of

Table 2
Formulation, physical characterization and thermodynamic stability of reconstituted ED-chitosan-S-PCN and Aerosil 200-S-PCN.

Formulation			
Code		ED-chitosan-S-PCN	Aerosil 200-S-PCN
Lipid phase (mL)	(Soyabean oil:Tween 80) (70:30)	0.395	0.375
Solid carrier (g)	ED-chitosan microparticles	1	–
	Aerosil 200	–	1
Drug (mg)	Primaquine	41	30
% Yield	S-PCN	98.43	97.12
Physical characterization			
Particle size (nm)		110	225
PDI		0.316	0.462
Zeta potential (mV)		0.1	11.3
Emulsification time (s)		28–32	60–65
Thermodynamic stability			
Cloud temperature (°C)		72	53
Centrifugation*	Phase separation	X	Y
	Precipitation	X	Y
Freeze–thaw cycle	4 °C	Clear	Clear
	40 °C	Clear	Clear

* X = No phase separation/Precipitation; Y = Phase separation/Precipitation.

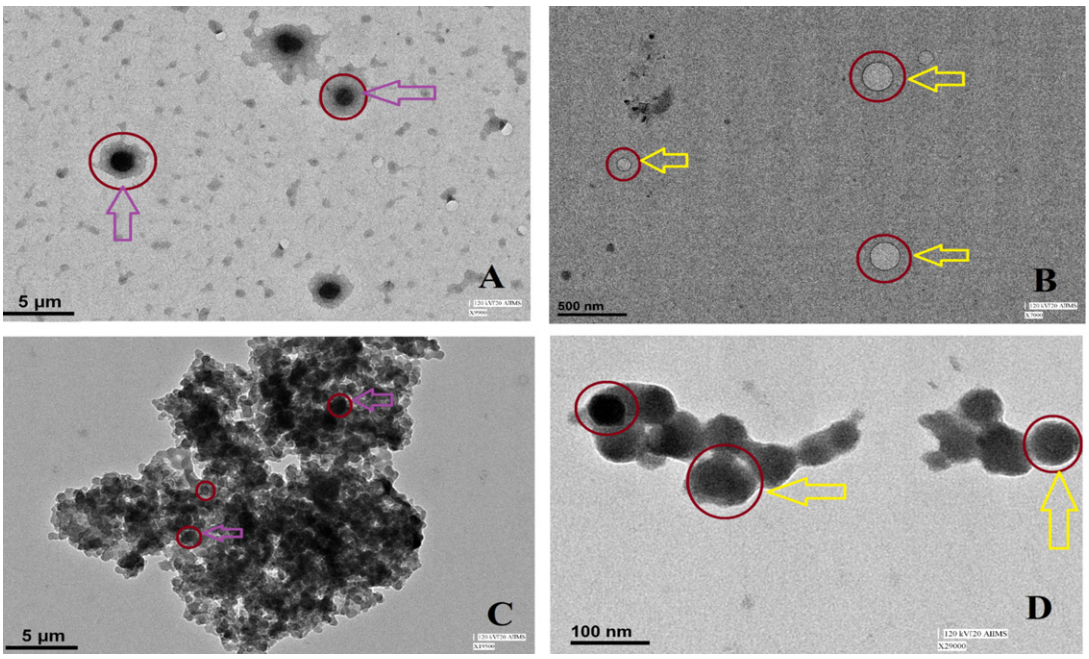

Fig. 7. Transmission electron micrographs: (A) ED-chitosan microparticles; (B) ED-chitosan-S-PCN; (C) Aerosil 200 (D) Aerosil 200-S-P-CN.

ED-chitosan in the fabrication of nanoemulsion containing primaquine.

3.6. *In vitro* drug dissolution study

An *in vitro* release performance of PQ incorporated into nanoemulsion was studied. A control nanoemulsion was studied. A control nanoemulsion containing PQ dissolved in soyabean oil:Tween 80 (70:30) in 80% (v/v) ethanol was prepared (L-PCN). The *in vitro* release of PQ from reconstituted nanoemulsion generated from ED-chitosan-S-PCN was found to be 80% within 10 min (Fig. 8A). This was similar to PQ release from L-PCN. However, just 10.75% was released from pure PQ sample. Thus, nearly 8-fold enhancement of dissolution behaviour of PQ was observed when incorporated into nanoemulsion prepared from ED-chitosan-S-PCN. Further, the release of PQ reconstituted nanoemulsion generated from Aerosil 200-S-PCN was 4 folds enhanced in comparison to PQ released from its pure form. than release from pure PQ. This suggested ED-chitosan could be used as a solid carrier to enhance dissolution behaviour and deliver lipid soluble drugs.

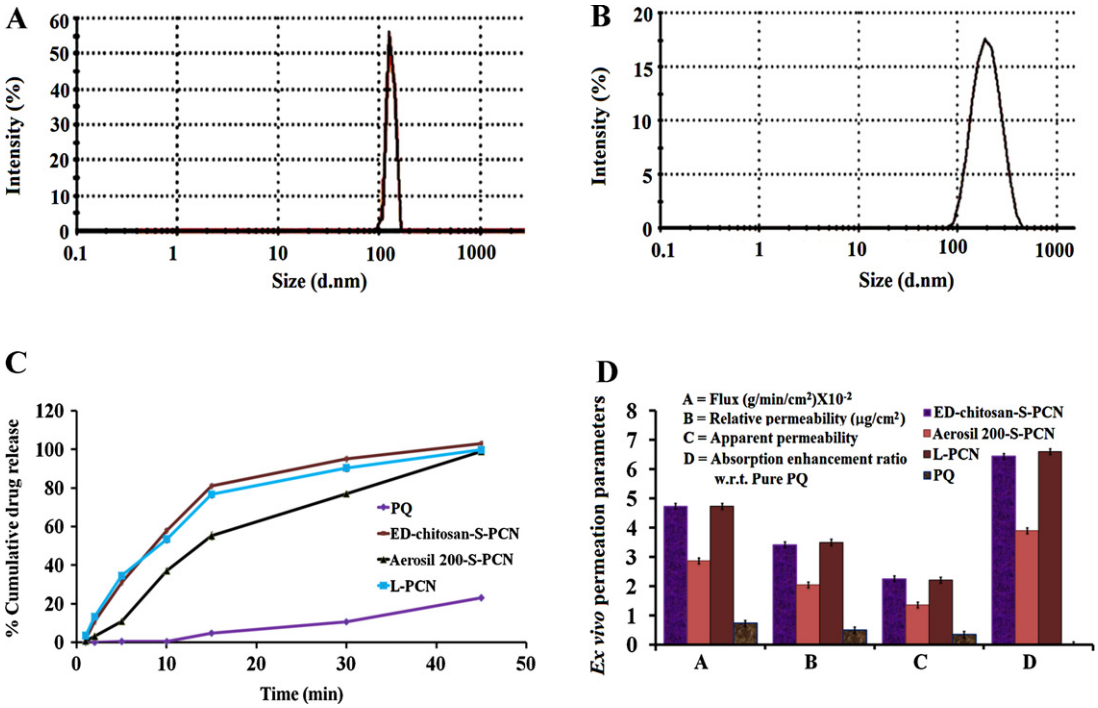

Fig. 8. (A) *In vitro* primaquine release from L-PCN (soyabean oil:Tween 80::70:30; 80%, v/v, ethanol), ED-chitosan-S-PCN and aerosil 200-S-PCN. (B) *Ex vivo* permeability evaluation of primaquine across porcine small intestine incorporated in ED-chitosan-S-PCN/Aerosil 200-S-PCN.

3.7. Ex vivo permeation studies

Ex vivo permeation studies were performed employing porcine small intestine method (Ghai & Sinha, 2012). The permeability of PQ from ED-chitosan-S-PCN was examined and compared with permeation of PQ from L-PCN or Aerosil 200-S-PCN. The results are summarized in Fig. 8B. The flux is an indicator of amount of drug permeated per unit area per unit time across a biological membrane. The higher flux suggested enhancement of drug permeation across membrane. The relative permeability suggested rate with which PQ transferred from serosal side of the intestine. The flux of PQ when released from ED-chitosan-SPCN was not significantly different ($P > 0.05$) from flux of PQ released from L-PCN. However, PQ obtained in the donor compartment when released from Aerosil 200-SPCN was significantly different ($P < 0.05$) than PQ entrapped into ED-chitosan-SPCN. Similar results were obtained with relative permeability and absorption enhancement ratio. Hence, the results suggested overwhelming influence of ED-chitosan as solid carrier in transporting lipid soluble drugs across biological membrane.

4. Conclusion

The current investigation pointed towards successful synthesis of ethylenediaminediacetic acid bis(carbido amide chitosan) without the use of proton initiator. The 3^2 full factorial design technique suggested 170 °C inlet temperature of spray drier as well as mixing of chitosan:EDTA in equal quantity as spraying solution produces highest yield of ED-chitosan. The FTIR-ATR and DSC analysis identified formation of amide linkages between NH_2 of chitosan and COO^- of EDTA-diNa along with presence of free acetate moieties. The synthesized ED-chitosan microparticles showed high oil desorbing capacity as compared to control chitosan microparticles and Aerosil 200. This was due to enhancement in the polar component of surface free energy of soyabean oil:Tween 80 (70:30) adsorbed ED-chitosan microparticles. The high soyabean oil:Tween 80 (70:30) carrying capacity of ED-chitosan could be associated with high dispersive component of surface free energy. This was also evident from SEM analysis. The high primaquine loading capacity of ED-chitosan-S-PCN as compared to Aerosil 200-S-PCN supported the potential of ED-chitosan in the fabrication of nanoemulsion. Further, the reconstituted nanoemulsion generated from ED-chitosan-S-PCN produces stable and smaller size nanoemulsion. Furthermore, the *in vitro* dissolution profile of PQ was 8 folds enhanced as compared to pure PQ when incorporated into ED-chitosan-S-PCN. This behaviour was also observed during *ex vivo* performance studies. Overall, the synthesis of ED-chitosan employing spray drying technology was simple and showed high level industrial potential in the fabrication of nanoemulsion.

Acknowledgements

The authors would like to acknowledge the financial assistance provided by UGC, New Delhi, under major research (File no. 39-168/2010 (SR) and CSIR, New Delhi (File no. 09/140(0154)/2010/EMR-I). We are also thankful to Director SAIF, AIIMS, New Delhi, for extending the facility of Transmission Electron Microscopy.

References

Alves, N. M., & Mano, J. F. (2008). Chitosan derivatives obtained by chemical modifications for biomedical and environmental applications. *International Journal of Biological Macromolecules*, *43*, 401–414.

Bachynsky, M. O., Shah, N. H., Patel, C. I., & Malick, A. W. (1997). Factors affecting the efficiency of a self-emulsifying oral delivery system. *Drug Development and Industrial Pharmacy*, *23*, 809–816.

Bandyopadhyay, S., Katare, O. P., & Singh, B. (2012). Optimized self nano-emulsifying systems of ezetimibe with enhanced bioavailability potential using long chain and medium chain triglycerides. *Colloids and Surfaces B: Biointerfaces*, *100*, 50–61.

Bernkop-Schnurch, A. (2000). Chitosan and its derivatives: Potential excipients for peroral peptide delivery systems. *International Journal of Pharmaceutics*, *194*, 1–13.

Bernkop-Schnurch, A., & Krajicek, M. E. (1998). Mucoadhesive polymers as platforms for peroral peptide delivery and absorption: Synthesis and evaluation of different chitosan-EDTA conjugates. *Journal of Controlled Release*, *50*, 215–223.

Bernkop-Schnurch, A., & Scerbe-Saiko, A. (1998). Synthesis and in vitro evaluation of chitosan-EDTA-protease-inhibitor conjugates which might be useful in oral delivery of peptides and proteins. *Pharmaceutical Research*, *15*, 263–269.

Cervera, M. F., Heinämäki, J., delaPaz, N., López, O., Maunu, S. L., Virtanen, T., et al. (2011). Effects of spray drying on physicochemical properties of chitosan acid salts. *AAPS PharmSciTech*, *12*, 637–649.

Chibowski, E., & Perea-Carpio, R. (2001). A novel method for surface free-energy determination of powdered solids. *Journal of Colloid and Interface Science*, *240*, 473–479.

Cho, Y. H., Kim, S., Bae, E. K., Mok, C. K., & Park, J. (2008). Formulation of a cosurfactant-free O/W microemulsion using nonionic surfactant mixtures. *Journal of Food Science*, *73*, E115–E121.

Cui, F., Shi, K., Zhang, L., Tao, A., & Kawashima, Y. (2006). Biodegradable nanoparticles loaded with insulin-phospholipid complex for oral delivery: Preparation, in vitro characterization and in vivo evaluation. *Journal of Controlled Release*, *114*, 242–250.

Elnaggar, Y. S. R., El-Massik, M. A., & Abdallah, O. Y. (2009). Self-nanoemulsifying drug delivery systems of tamoxifen citrate: Design and optimization. *International Journal of Pharmaceutics*, *380*, 133–141.

El-Sharif, A. A., & Hussain, M. H. M. (2011). Chitosan–EDTA new combination is a promising candidate for treatment of bacterial and fungal infections. *Current Microbiology*, *62*, 739–745.

Ferrari, P. C., Souza, F. M., Giorgetti, L., Oliveira, G. F., Ferraz, H. G., Chaud, M. V., et al. (2013). Development and in vitro evaluation of coated pellets containing chitosan to potential colonic drug delivery. *Carbohydrate Polymers*, *91*, 244–252.

Ghai, D., & Sinha, V. R. (2012). Nanoemulsions as self-emulsified drug delivery carriers for enhanced permeability of the poorly water-soluble selective β_1-adrenoreceptor blocker talinolol. *Nanomedicine*, *8*, 618–626.

Jindal, M., Kumar, V., Rana, V., & Tiwary, A. K. (2013). Physico-chemical, mechanical and electrical performance of bael fruit gum-chitosan IPN films. *Food Hydrocolloids*, *30*, 192–199, 2012.

Kang, J. H., Oh, D. H., Oh, Y. K., Yong, C. S., & Choi, H. G. (2012). Effects of solid carriers on the crystalline properties, dissolution and bioavailability of flurbiprofen in solid self-nanoemulsifying drug delivery system (solid SNEDDS). *European Journal of Pharmaceutics and Biopharmaceutics*, *2*, 289–297.

Kumar, M. N., Muzzarelli, R. A. A., Muzzarelli, C., Sashiwa, H., & Domb, A. J. (2004). Chitosan chemistry and pharmaceutical perspectives. *Chemical Reviews*, *104*, 6017–6084.

Loretz, B., & Bernkop-Schnürch, A. (2006). In vitro evaluation of chitosan-EDTA conjugate polyplexes as a nanoparticulate gene delivery system. *The AAPS Journal*, *8*, E756–E764.

Matsumaru, H. (1959). Tablet disintegration by surface tension. *Yakugaku Zasshi*, *79*, 854–855.

Mehta, S. K., Kaur, G., & Bhasin, K. K. (2010). Tween-embedded microemulsions—Physicochemical and spectroscopic analysis for antitubercular drugs. *AAPS PharmSciTech*, *11*, 143–153.

Mohajel, N., Najafabadi, A., Azadmanesh, R., Vatanara, K., Moazeni, A., Rahimid, E., et al. (2012). Optimization of a spray drying process to prepare dry powder microparticles containing plasmid nanocomplex. *International Journal of Pharmaceutics*, *423*, 577–585.

Muzzarelli, R. A. A. (2009). Genipin-crosslinked chitosan hydrogels as biomedical and pharmaceutical aids. *Carbohydrate Polymers*, *77*, 1–9.

Muzzarelli, R. A. A., & Ilari, P. (1994). Chitosans carrying the methoxyphenyl functions typical of lignin. *Carbohydrate Polymers*, *23*, 155–160.

Muzzarelli, C., Stani, V., Gobbi, L., Tosi, G., & Muzzarelli, R. A. A. (2004). Spray drying of solutions containing chitosan together with polyuronans and characterization of the microspheres. *Carbohydrate Polymers*, *57*, 73–82.

Muzzarelli, R. A. A., Boudrant, J., Meyer, D., Mannod, N., DeMarchis, M., & Paoletti, M. G. (2012). Current views on fungal chitin/chitosan, human chitinases, food preservation, glucans, pectins and inulin: A tribute to Henri Braconnot, precursor of the carbohydrate polymers science, on the chitin bicentennial. *Carbohydrate Polymers*, *87*, 995–1012.

Muzzarelli, R. A. A., Greco, F., Busilacchi, A., Sollazzo, V., & Gigante, A. (2012). Chitosan, hyaluronan and chondroitin sulfate in tissue engineering for cartilage regeneration: A review. *Carbohydrate Polymers*, *89*, 723–739.

Planinsek, O., Kovacic, B., & Vrecer, F. (2011). Carvedilol dissolution improvement by preparation of solid dispersions with porous silica. *International Journal of Pharmaceutics*, *406*, 41–48.

Qu, X., Wirsen, A., & Albertsson, A. C. (1999). Synthesis and characterization of pH-sensitive hydrogels based on chitosan and D,L-lactic acid. *Journal of Applied Polymer Science*, *74*, 3193–3202.

Rai, P., Tiwary, A. K., & Rana, V. (2012). Superior disintegrating properties of calcium cross-linked Cassia fistula gum derivatives for fast dissolving tablets. *Carbohydrate Polymers*, *87*, 1098–1104.

Rana, V., Rai, P., Tiwary, A. K., Singh, R. S., Kennedy, J. F., & Knill, C. J. (2011). Modified gums: Approaches and applications in drug delivery. *Carbohydrate Polymers*, *83*, 031–1047.

Rattes, A. L. R., & Oliveira, W. P. (2007). Spray drying conditions and encapsulating composition effects on formation and properties of sodium diclofenac microparticles. *Powder Technology*, *171*, 7–14.

Rege, P. R., Garmise, R. J., & Block, L. H. (2003a). Spray-dried chitosans. Part I: Preparation and characterization. *International Journal of Pharmacy*, *252*, 41–51.

Rege, P. R., Garmise, R. J., & Block, L. H. (2003b). Spray-dried chitosans. Part II: In vitro drug release from tablets made from spray-dried chitosans. *International Journal of Pharmacy*, *252*, 53–59.

Schafroth, N., Arpagaus, C., Jadhav, U. Y., Makne, S., & Douroumis, D. (2012). Nano and microparticle engineering of water insoluble drugs using a novel spray-drying process. *Colloids and Surfaces B: Biointerfaces*, *90*, 8–15.

Shah, S., & Thassu, D. (2005). Disodium edetate. In R. C. Rowe, P. J. Sheskey, & M. E. Quinn (Eds.), *Handbook of pharmaceutical excipients* (6th ed., pp. 242–243). London: Pharmaceutical Press.

Shanmugam, S., Baskaran, R., Balakrishnan, P., Thapa, P., Yong, C. S., & Yoo, B. K. (2011). Solid self-nanoemulsifying drug delivery system (S-SNEDDS) containing phosphatidylcholine for enhanced bioavailability of highly lipophilic bioactive carotenoid lutein. *European Journal of Pharmaceutics and Biopharmaceutics*, *79*, 250–257.

Singh, K. K., & Vingkar, S. K. (2008). Formulation, antimalarial activity and biodistribution of oral lipid nanoemulsion of primaquine. *International Journal of Pharmaceutics*, *347*, 136–143.

Singh, K., Suri, R., Tiwary, A. K., & Rana, V. (2012). Chitosan films: Crosslinking with EDTA modifies physicochemical and mechanical properties. *Journal of Material Science: Material in Medicine*, *23*, 687–695.

Tang, B., Cheng, G., Gu, J. C., & Xu, C. H. (2008). Development of solid self-emulsifying drug delivery systems: Preparation techniques and dosage forms. *Drug Discovery Today*, *13*, 606–612.

Yoshihashi, Y., Makita, M., Yamamura, S., Fukuoka, E., & Terada, K. (1998). Measurement of rates of water penetration into tablets by microcalorimetry. *Chemical & Pharmaceutical Bulletin*, *46*, 437–477.